International Journal for Housing Science and Its Applications
Publish August 5, 2025. Volume 46, Issue 3 Pages 4327-4339

https://doi.org/10.70517/ijhsa463370

# Study on multi-area protection coordination of AC-DC hybrid power systems based on distributed computing

**Wei Xu[1], Yu Sui[1,*], Yabin Chen[1] and Huazhen Cao[1]**
[1] Power Grid Planning Research Center of Guangdong Power Grid Co., Ltd., Guangzhou, Guangdong, 510220, China
Corresponding authors: (e-mail: SuiYu202412@126.com).

**Abstract** With HV/EHV DC transmission gradually becoming the main mode of regional power grid interconnection, the problem of multiregional protection coordination of AC/DC hybrid power systems has become an important issue that needs to be concerned and solved. Based on the relevant theoretical knowledge and simulation platform, the AC/DC hybrid power system is designed, and then the multi-area protection coordination problem of the system is converted into a nonlinear planning problem by combining the concept and characteristics of distributed computing. Based on the objective function, constraints, and optimized particle swarm algorithm, to design the multi-area protection coordination scheme of AC/DC hybrid power system, and the scheme is empirically analyzed. The optimal protection coordination time of the AC/DC hybrid power system with the introduction of distributed generation equipment is 2.531s, i.e., after the optimization of the algorithm in this paper, the protection coordination performance of the system is further optimized, so that the system can better serve the electricity customers.

**Index Terms** distributed computing, optimized particle swarm algorithm, power system, protection coordination

## I. Introduction

At present, the distribution networks at home and abroad are still dominated by the traditional AC power distribution method. With the emergence of various types of DC loads and electronic loads, a large number of DC switching power supplies as well as frequency converters have been applied in practice, and the existing urban power distribution is no longer a pure AC power distribution method [1], [2]. The DC power distribution method shows the advantages that the traditional AC power distribution method does not have in terms of consuming distributed energy, improving energy utilization efficiency and power quality as well as compatibility with a large number of current DC loads and inverter appliances [3]-[5]. However, because the traditional AC power distribution method has accumulated a large amount of technology, equipment, and assets in decades of application history, DC power distribution method has great advantages in many aspects, but it is not realistic to completely replace the AC power distribution method [6]-[8]. Therefore, from the perspective of fully utilizing the assets stored in the original AC power distribution system and the advantages of DC power distribution system, AC/DC hybrid power distribution method is likely to become the mainstream form of power distribution system in the future [9].

At present, China has formed the basic pattern of AC/DC hybrid power system with high voltage level and long-distance transmission, which improves the ability of optimizing the allocation of resources in a wide range and guaranteeing the power demand of different regional loads [10], [11]. However, at the same time, it also makes the operation of the power grid face many difficult challenges. Compared with the traditional AC power grid, the grid structure of AC-DC hybrid power grid has been greatly changed, the coupling relationship between various parts is closer, and the constraints that need to be satisfied to realize normal operation are also more complicated, which exacerbates the risk of chain failures of the hybrid power system [12]-[15]. From this point of view, the study of multi-area protection coordination strategies for AC-DC hybrid power systems is conducive to ensuring the safe and stable operation of power grids [16], [17].

With the support of the simulation platform, the design of the AC/DC hybrid power system is accomplished from the two parts of AC system and DC system. Within the scope of distributed computing theory, the AC/DC hybrid power system multi-area protection coordination problem can be regarded as a mixed integer nonlinear programming problem, then set the objective function and constraints, and use the optimized particle swarm algorithm as the model optimization solution algorithm, so as to formulate an AC/DC hybrid power system multi-area protection coordination scheme based on the optimized particle swarm algorithm. Combining the above models and algorithms, the research scheme of this paper is empirically analyzed from three aspects: algorithm validation, model solving, and actual cases.

# II. AC/DC hybrid power system modeling

## *II. A. Components of AC/DC hybrid power systems*

The structure of the whole system is shown in Fig. 1. In this paper, an AC/DC hybrid power system model is constructed on the simulation platform based on an actual AC transmission project and a high-voltage DC transmission project. units 1 and 2 (2×500MW) and units 3 and 4 (2×600MW) are connected to a transformer substation via a double 500kV AC transmission line, and then connected to an infinite power grid via three 500kV AC transmission lines. Infinity power grid. The total length of the double-back AC transmission line is 378km, the total length of the triple-back AC transmission line is 108km, and ±500kV bipolar DC transmission lines are connected in parallel at both ends of the AC transmission line.

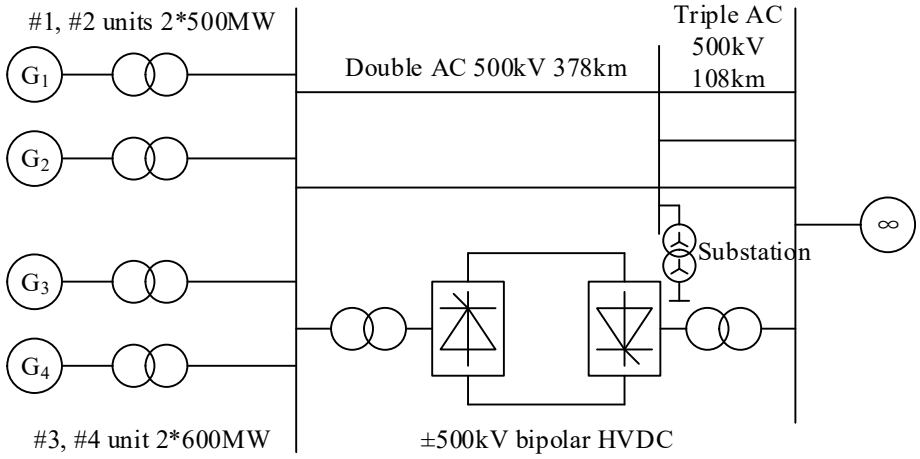


Figure 1: Structure of AC/DC hybrid power system

### II. A. 1) Communication systems

The AC system part mainly consists of turbine generator sets, AC transmission lines, series compensation capacitors and equivalent power grids.

(1) Turbine generator sets

The AC/DC transmission project consists of four turbine-generator sets in one and two phases of a power plant at the sending end. The shaft system of No.1 and No.2 units in the first phase adopts the centralized parametric model of six-mass block elastic shaft, and the intrinsic torsional vibration modal frequencies of the shaft system are 14.944 Hz, 27.403 Hz, 31.52 Hz, 37.361 Hz and 49.601 Hz respectively.

(2) AC transmission line

The total length of the double-circuit AC transmission line is 378km, of which one circuit (Line A) has two sets of 150Mvar high reactance on the generator side and one set of 150Mvar high reactance on the substation side. The other one (line B) has 1 group of 150Mvar high reactance on the generator set side and 2 groups of 150Mvar high reactance on the substation side. The total length of the three AC transmission lines is 108km. the fixed load model in the standard component library is used to simulate the shunt high reactance compensation in the transmission lines.

(3) Series compensation capacitor

The series capacitor compensation in the double circuit line consists of two parts: fixed series compensation and controllable series compensation. Fixed series compensation is composed of a capacitor with fixed parameters and a protection element in parallel for each phase. The capacitor model in the standard component library is used to simulate the fixed series compensation capacitance, and the capacitor parameters are set so that the capacitive reactance at industrial frequency is 30% of the total reactance of the line in which it is located, and the MOV protection level is set to 2.3 p.u. The capacitor model is used to simulate the fixed series compensation capacitance. The controlled series complement (TCSC) sets the parameters of each component so that when the thyristor cuts off, the capacitor itself produces a compensating reactance of approximately 15% of the total reactance of the transmission line on which it is located.

(4) Equivalent grid

The units on the 500kV grid in the area where the substation is located are simulated by an equivalent generator, which is connected to the 500kV bus of the substation through two step-up transformers. The fixed load model in

the standard component library is used to simulate the local load, and the load type is impedance type. The unit output and load fluctuation range of the 220kV grid in this area is set as 0~1800MW.

**II. A. 2) DC systems**

The DC transmission project is a bipolar operation structure, the converter station adopts 12-pulse wave converter, the rated capacity of DC transmission is bipolar 1000MW, the rated operating voltage is ±500kV, the rated operating current is 1kA, and the length of the line is 486km. filters and shunt capacitors are used for the reactive compensation of the line, and the total capacity of rectifier-side reactive compensation is 400Mvar, while the total capacity of inverter-side reactive power compensation is 600Mvar. The total capacity of rectifier-side reactive power compensation is 400 Mvar, and that of inverter-side reactive power compensation is 600 Mvar. The principle wiring of the DC transmission project is shown in Fig. 2. The DC transmission system is mainly composed of converter, converter transformer, AC/DC filter, leveling reactor and reactive power compensation.

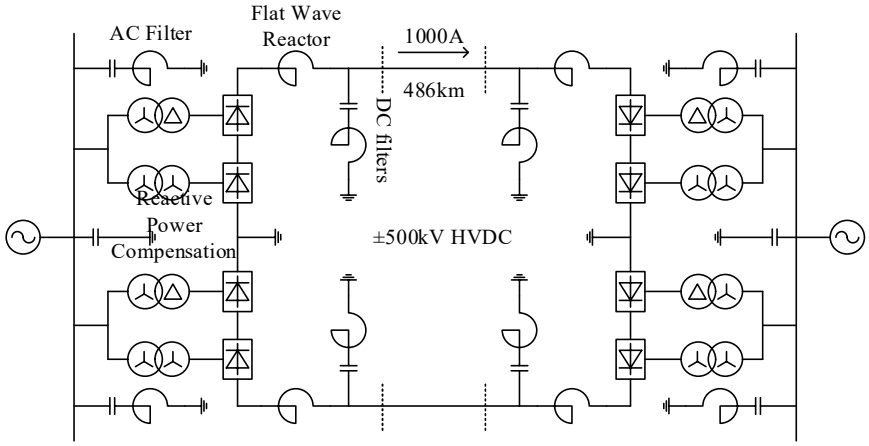


Figure 2: Principle wiring diagram of DC transmission project

***II. B.Excitation regulator and power system stabilizer modeling***

Figure 3 shows the block diagram of the excitation regulator transfer function, the excitation regulation system is an important part of the synchronous motor, generally consists of two parts: the excitation power unit and the excitation regulator, the excitation power unit is responsible for providing stable and reliable DC excitation current to the excitation winding in the motor, and the excitation regulator automatically adjusts the size of the excitation current output from the excitation power unit in accordance with the requirements of the motor and system operation. Under certain conditions, the phase lag characteristics of the excitation regulation system and the motor excitation winding may cause the voltage regulator to produce a negative damping torque that is phase lagged behind the power angle and inversely proportional to the change in rotational speed, and when the voltage regulator is overly sensitive, the system may oscillate. The power system stabilizer provides an additional signal to the excitation regulation system, which, after phase compensation, causes it to produce a positive damping torque to suppress system oscillations.

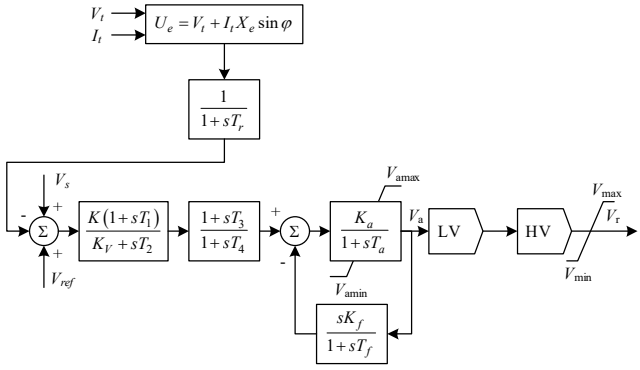


Figure 3: Block diagram of the transfer function of the excitation modulator

### *II. C.DC converter station modeling*

The converter station consists of a converter transformer and a converter valve bridge. The positive and negative poles of the DC system each have a 12-pulse rectifier bridge and a 12-pulse inverter bridge, and each 12-pulse converter bridge consists of two 6-pulse three-phase fully controlled converter bridges connected in series. Each 6-pulse converter bridge corresponds to a converter transformer. The three-phase two-winding transformer model in the PSCAD standard component library is used to simulate the converter transformer, and the 6-pulse bridge model is used to simulate the 6-pulse three-phase fully-controlled converter bridge.

### *II. D.AC/DC Filter Modeling*

AC and DC filters are passive filters, that is, composed of capacitors and inductors and other components, component parameters in accordance with the converter station generated by the characteristic harmonics of the various settings, so that the filter in the corresponding characteristic frequency of the narrow range of resonance, presenting a low impedance state, in order to achieve the purpose of eliminating harmonics.

### *II. E.DC control system modeling*

DC voltage, current and delivered power can be controlled in a DC system by controlling the trigger delay angle $\alpha$ of the rectifier and the inversion angle $\beta$ of the inverter. The rectifier side usually adopts the constant current control method, the constraint equation is $I_d = I_{ds}$ ( $I_d$ is the DC current, $I_{ds}$ is the given value), and the adjustment $\alpha$ makes the deviation of the DC current from the given value tends to zero, so as to achieve the purpose of control. The inverter side usually adopts constant arc quenching angle control or constant voltage control mode, and the constraint equations are $\delta_d = \delta_s$ ( $\delta_s$ is the given value) and $U_{di} = U_{dis}$ ( $U_{dis}$ is the given value), respectively, and the constant arc quenching angle control mode ensures the reliable shutdown of the thyristor. In addition, both the rectifier side and the inverter side have low voltage current limiting (VDCOL) control links.

In this DC project, constant current control is used on the rectifier side, and constant current control and constant shut-off angle control are used on the inverter side. The shut-off angle $\gamma = \pi -$ arc quenching angle $\delta$, and the minimum value of the measured angle of the inverter side in the last cycle $\gamma$ is taken as the input quantity. Both the constant current control and constant turn-off angle control strategies use a PI controller, and the output of the PI controller is the trigger overrun angle $\beta$, where $\beta = \pi - \alpha$. After processing, the output is the $\alpha$ angle command for the rectifier side and the inverter side. At any moment, only one of the two control strategies on the inverter side is selected. According to the operating characteristics of the inverter, the two outputs are selected by taking the maximum value, and after conversion, the trigger delay angle $\alpha$ command on the inverter side is obtained. The function of the current deviation control link is to enable the system to make a smooth transition between the two ways of inverter-side constant current and constant off angle control to avoid the uncertainty and back and forth swing of the control strategy, which does not work under normal operating conditions.

## III. Systematic multi-regional protection coordination

### *III. A. Introduction to Distributed Computing*

#### III. A. 1) Concepts of Distributed Computing

Distributed computing is a computer science discipline that has been proposed in recent years as a new way of computing, which investigates how to divide a problem that requires a very large amount of computational power to solve into many small parts [18]. These parts are then distributed to many computers for processing, and finally the results of these computations are synthesized to get the final result [19]. Distributed computing requires sharing information with each other on two or more pieces of software that can either run on the same computer or on multiple computers connected through a network.

#### III. A. 2) Characteristics of Distributed Computing

The application requirements of high-performance computing make it impossible to obtain computing power on a single computer, so it is necessary to construct a “networked virtual supercomputer” or “metacomputer” to obtain super computing power. Meta-computing is defined as the connection of powerful computing resources through the network to form a supercomputing environment that is transparent to the user, and it realizes a supercomputing environment by connecting geographically distributed computers of various types (including clusters), databases, various types of devices, and storage devices through the network. Distributed computing has several advantages over other algorithms:

(1) Rare resources can be shared.

(2) Distributed computing can balance the computational load on multiple computers.

(3) A program can be placed on the computer best suited to run it.

Among them, sharing scarce resources and balancing loads are one of the core ideas of distributed computing. If we say that a certain work is distributed, then, to participate in this work must be not only a computer, but a computer network, obviously this “ants moving mountains” will have a very strong data processing capabilities, the essence of distributed computing is to combine and share resources and ensure system security.

### *III. B. Design of the system's multiregional protection coordination program*

Multi-area protection coordination of AC and DC power systems based on distributed computing is most concerned with deciding the objective function, decision variables and constraints. The optimization objective of the AC/DC power system multi-area protection coordination problem is first discussed, and the system protection coordination problem is equated into a mixed-integer nonlinear programming problem, which gives the optimization objective function and the mathematical model of the AC/DC power system characteristics, as well as its associated constraints on the system characteristics. Simple optimization models are often one- or multivariate unconstrained or equation-constrained optimization problems. In many practical problems, the values of the decision variables that can be provided are constrained by a number of factors, which gives rise to general optimization models, collectively known as mathematical planning models. Details are given below:

#### III. B. 1) Description of the problem

The so-called multi-area protection coordination of AC and DC power systems is to find a set of parameter values, under certain constraints, so that certain optimality measures are satisfied and certain performance indexes of the system are maximized or minimized. In general, let the optimization problem under consideration be:

$$\min \sigma = f(x) \quad X \in S = \{X \mid g_i(x) \le 0, j = 1,2,\cdots,m\} \tag{1}$$

where $\sigma = f(x)$ is the objective function, $g_i(x)$ is the constraint function, $S$ is the constraint domain, and $X$ is the $n$-dimensional optimization variable. Usually the maximization problem is easily converted to a minimization problem $\sigma = -f(x)$, and the constraints and equational constraints for $g_i(x) \ge 0$ can also be converted to constraints for $-g_i(x) \le 0$, so that the optimization problem described does not lose its generality. When $f(x)$, $g_i(x)$ are linear functions and $X \ge 0$, the optimization problem described above is a linear programming problem, and its solution method is particle swarm algorithm. When at least one of $f(x)$, $g_i(x)$ is a nonlinear function, the above problem is a nonlinear programming problem.

#### III. B. 2) Objective function

In order to overcome the difficulties of the traditional AC/DC power system multi-area protection coordination and cooperation calculation method in practical application, this paper establishes an optimization model according to the specific requirements of the AC/DC power system multi-area protection, with the expected value of AC/DC power system multi-area protection action time and fault duration as the optimization objectives, and the set value of the system characteristic parameter in the system as the decision variable. Then the particle swarm optimization algorithm is used to solve the optimization model in order to achieve the purpose of minimizing the coordination time of multi-area protection of AC and DC power systems. In this paper, we focus on the reasonable selection of the starting current value of the multi-area protection of AC and DC power systems, equate the problem of system multi-area protection coordination into a mixed integer nonlinear programming (MINLP) problem, and calculate the system action time value, with the goal of minimizing the overall action time of the system. The system time coordination problem in the system protection coordination problem can be established as the following objective function:

$$\min \sum W_{i'} T_{i,k} \tag{2}$$

where $W_{i'}$ denotes the likelihood of a fault occurring on the line, which is usually set to 1. $T_{i,k}$ denotes the action time of the system $R_i$ when a fault occurs in region $k$. Namely:

$$\min\left(\alpha \cdot \sum W_{i'} T_{i,k} + \beta \cdot \sum_k (\tau_k \cdot P_k)\right) \tag{3}$$

The weighted average of the above 2 indicators is taken as the overall objective function, where $\alpha$ and $\beta$ are the weighting coefficients, which represent the degree of preference for the 2 indicators in the coordinated

computation process, and can be set differently for different fault situations according to different power system optimization problems.

The objective function needs to satisfy the minimum action time in the whole system in addition to maximizing the requirements of all system main and backup protections, and satisfy all the constraints proposed by the algorithm in this paper.

**III. B. 3) Constraints**

(1) The relationship between the system's primary and backup protection time coordination:

$$T_{j,k} - T_{i,k} \geq \Delta T \tag{4}$$

where $T_{j,k}$ denotes the action time of the backup protection system $R_j$ configured for the system $R_i$. The $\Delta T$ denotes the protection level difference time.

(2) System fit pair constraint coefficients $M_{i,j}$:

$$M_{i,j} = \begin{cases} 1, & \Delta T < \delta \\ 0, & \Delta T > \delta \end{cases} \tag{5}$$

where $\delta$ is the actual system protection level difference time, the total number of constraint violations for all system fit pairs in all faults is $\sum\sum M_{i,j}$. If the value of $\sum\sum M_{i,j}$ is 0, it means that the result of the rectification is able to guarantee the selectivity of the protection equipment action for all fault cases, which is the best result of the rectification calculation.

In the case of guaranteeing greater than the time level difference, in order to protect the quick action of the equipment, the time difference of the matching pair action should be as small as possible. Various fault conditions in the mutual cooperation of protection equipment action time difference and the difference between the time with the difference between the sum of the level as a minimization of the objective function, should be the DC power system for multi-area protection coordination must be taken into account.

(3) Constraints on system rectification time coefficients and action times:

$$TDS_{i_{\min}} \leq TDS_i \leq TDS_{i_{\max}} \tag{6}$$

$$T_{i_{\min}} \leq T_i \leq T_{i_{\max}} \tag{7}$$

where $T_i$ denotes the action time of the system $R_i$ in the event of a fault in region $k$, and the $TDS_i$ upper and lower limits of the time coefficients are usually 0.1 and 11, respectively.

(4) Constraints on starting current:

$$I_{pi_{\min}} \leq I_{pi} \leq I_{pi_{\max}} \tag{8}$$

where the magnitude of the system starting current $I_p$ varies with the characteristics and specifics of the protective device.

**III. B. 4) Model solving based on optimized particle swarm algorithm**

(1) The optimized particle swarm algorithm is initialized by introducing the following rules:

$$x_{\max} = (x_{\max} - x_{\min}) \times r + x_{\max} \tag{9}$$

$$v_{\max} = (v_{\max} - v_{\min}) \times r + v_{\min} \tag{10}$$

where $x_{\max}$, $x_{\min}$ denote the maximum and minimum values of the particle position movement in each iteration, $v_{\max}$, $v_{\min}$ denote the maximum and minimum values of the particle velocity in each iteration, and $r$ is a random value between 0 and 1. Under the premise of satisfying some of the constraints, initialize the appropriate solution of the particle part according to Eq. Determine the dimensions of the optimization variables, and set the particle swarm size and algorithm parameters, i.e., the learning factor, the speed limit, and so on. Set the maximum number of iterations. The position of each particle represents a possible set of computational results, i.e., each particle contains all the computational information determined. For each of the previously mentioned protection segments, its fit state with neighboring protections can be represented by binary characters of a certain length, and connecting the individual characters constitutes the basic information of a particle in the population.

(2) Calculate the fitness value of each particle. It is as follows:

$$fit = \frac{1}{\sum T_{i,k}}\left(1-\sum_{1}^{m} n_m\right) \tag{11}$$

where $fit$ denotes the fitness value of the particle, $m$ denotes the number of constraints, and $n$ denotes the threshold value at the current constraint. When all constraints are satisfied, the value of $n$ is taken as 0. When the obtained solution is not suitable, the value of $n$ is taken as 1. For the objective function mentioned in Chapter 2, it is important to satisfy the constraints that there is a minimum action time for the whole protection as well as maximizing the satisfaction of all protections.

(3) Calculate the value of the historical optimal point fitness function for each particle and compare it with the current fitness function value for each particle. If the current fitness function value of the particle is greater than the fitness function value of its historical optimum, the historical optimum position of the particle is replaced with the current position and the historical optimum fitness function value is replaced with the current fitness function value. The current optimal point of the population is compared to the fitness function value of the historical optimal point, and if the fitness function value of the current optimal point of the population is greater than the fitness function value of the historical optimal point, the historical optimal position of the population is replaced with the current position of the optimal particle of the population, and the historical optimal fitness function value of the population is replaced with the fitness function value of the current optimal particle.

## IV. Empirical analysis of protection coordination in multiple regions of the system

### *IV. A. Algorithm Validation Analysis*

#### IV. A. 1) Analytical notes

Some test functions are selected to assess the performance of the optimized particle swarm algorithm proposed in this paper, and when selecting these functions, it is necessary to consider the various mathematical characteristics and influencing factors of the mathematical model established on the basis of the actual application problem. In summary, the main characteristics of the function are: the continuity of the function, concavity and convexity, the dimensionality of the function, the certainty and randomness of the function, and the number of peaks of the function. In this paper, the following two standard test functions are selected to test the performance of the optimized particle swarm algorithm, which are carefully designed and rigorously tested. If the optimized particle swarm algorithm can solve the problem represented by a certain test function well, it can be assumed that it will also have a better performance in a large number of other practical problems, which will verify the effectiveness of this paper's algorithm in the coordination of multiregional protection of power systems. Application of this paper's algorithm in power system multi-area protection coordination.

#### IV. A. 2) Analysis of results

The test function A has an extremely large number of very deep local optima arranged by sinusoidal inflection points, and the global optimal solution is obtained at $x=\{0,0,\cdots,0\}$, at which point $f(x)=0$. The optimization algorithm can easily fall into the local optimal point in the process of searching for the global optimal point, which is a very difficult function to optimize, and the simulation analysis of the test function A is shown in Figure 4. The global optimum points obtained by the standard particle swarm algorithm (PSO), genetic algorithm (GA), simulated annealing algorithm (SA) and optimized particle swarm algorithm (IPSO) optimization of the test function A are shown in Fig. 5, and the dimensionality of the function is 20, and in order to reduce the chance of the results of a single simulation test, the number of simulation tests is set to ten. It can be seen that although the standard quantum particle swarm algorithm occasionally searches for a better solution than the other algorithms in one or two 1 trials, but in general, the overall performance of the other three is more stable and better, and at the end of the ten trials, focusing on the one that obtained the lowest adaptation value, it is found that the optimal solutions obtained by the other three algorithms are closer to the global optimum than those searched for by the standard particle swarm algorithm $f(x)=0$. This indicates the effectiveness of the algorithmic improvements. For the test function A, the most satisfactory optimization performance is the optimized particle swarm algorithm in this paper.

The test function B is a nonlinear strongly multi-peaked function with strong correlation between the variables, so the optimization algorithm can easily fall into the local optimum, and the global optimal solution of the function is obtained at $x=\{0,0,\cdots,0\}$, when $f(x)=0$. As the dimensionality of the function increases, the influence of the cumulative part of the function becomes smaller, and the region of the local optimum becomes smaller and smaller, so that searching for the global optimum point becomes relatively easy instead. The test function B is 30-dimensional, but it is easier to find the global optimum point by the particle swarm algorithm than the 10-dimensional and 20-

dimensional test function B. The local graph of the function is shown in Fig. 6. The global optimal point obtained by different algorithms for optimization of test function B is shown in Fig. 7, with a function of dimension 20. Again, the number of simulation trials is set to ten in order to reduce chance. As can be seen from the figure below, the optimal solutions obtained by the particle swarm algorithm and the other three algorithms are very close to the global optimum $f(x)=0$, and it is also found that the optimal solutions of the other three algorithms are below that of the particle swarm algorithm in most of the trials. For test function B, the optimal search performance is more desirable also for the optimized particle swarm algorithm. It is important to note that improved algorithms that achieve better performance in individual test functions do not represent optimal performance in general. In addition, the average performance basically represents the convergence speed of the algorithm, but does not indicate whether it is more likely to approach the global optimum. On some multi-peaked functions, the algorithm is also able to obtain better adaptation values if the best local optimum region is often found. In fact, if there is no limit to the number of times the algorithm can be executed, a more reasonable metric would be to look at the one solution that gets the best after a certain number of trials of function evaluation.

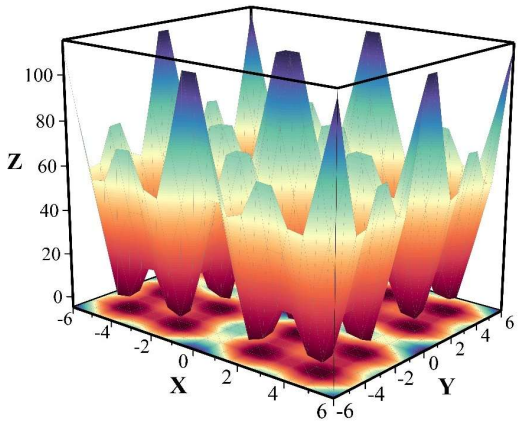


Figure 4: Test function A simulation analysis

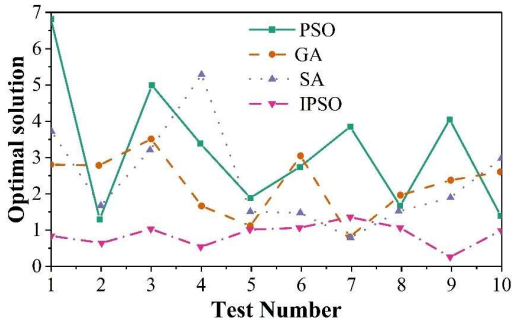


Figure 5: Comparison of the optimization performance of functions A

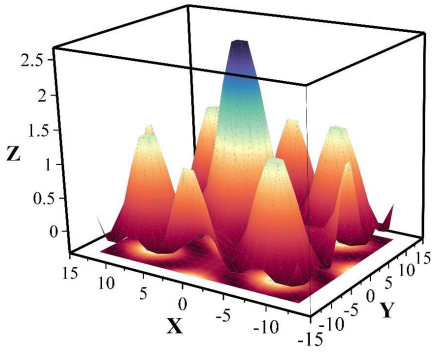


Figure 6: Test function B simulation analysis

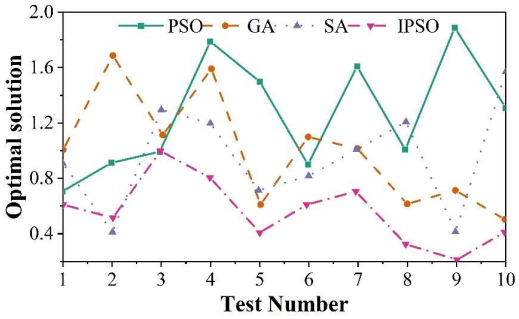


Figure 7: Comparison of the optimization performance of functions B

### *IV. B. Model Solution Analysis*

#### IV. B. 1) Parameter setting

Taking the IEEE-33 AC/DC hybrid power system as an example, the maximum number of iterations of the integer particle swarm is set $G_{\max}=100$, the population data $N=100$, $w=0.7$, $c_1=1.4$, $c_2=1.4$, and the contraction factor for $IPSO$ is $\beta=0.60$, and the initial speed is 0. Four nodes are selected at the system backbone nodes to access the distributed generation units (DGs), and the optimization settings are set such that each DG output is between 0 and 1 MW at 0.1 MW intervals.

#### IV. B. 2) Analysis of solution results

Fig. 8 shows the simulation diagram of DG access position based on PSO algorithm, and Fig. 9 shows the simulation diagram of DG access position based on IPSO algorithm, the comparison of the parameters of the comprehensive optimization after system access to DG is shown in Table 1, the comparison of the iterative convergence of system access to DG is shown in Fig. 10, and the comparison of the protection coordination time of the system after access to DG is shown in Fig. 11. The comprehensive charts show that after the algorithm optimization of AC/DC hybrid power system multi-area protection coordination, the network loss is much lower than the pre-optimization and PSO algorithms, and the AC/DC hybrid power system multi-area protection coordination time is reduced, and the effect of the system multi-area protection coordination is more rapid and stable, and the feasibility of the algorithm optimization has been verified at the same time.

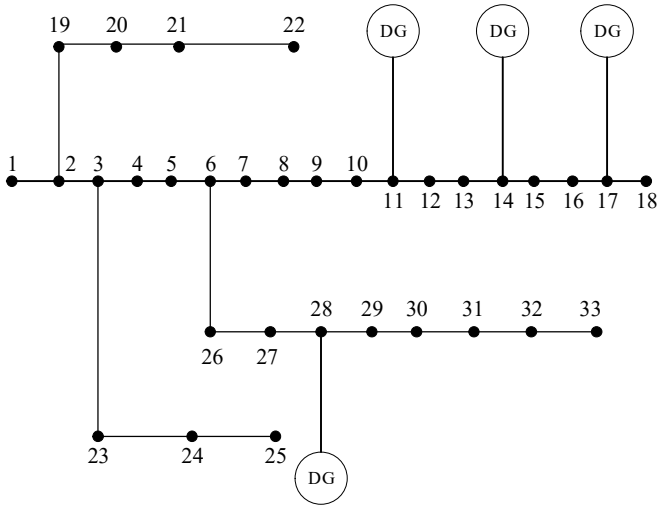


Figure 8: DG access location based on PSO algorithm

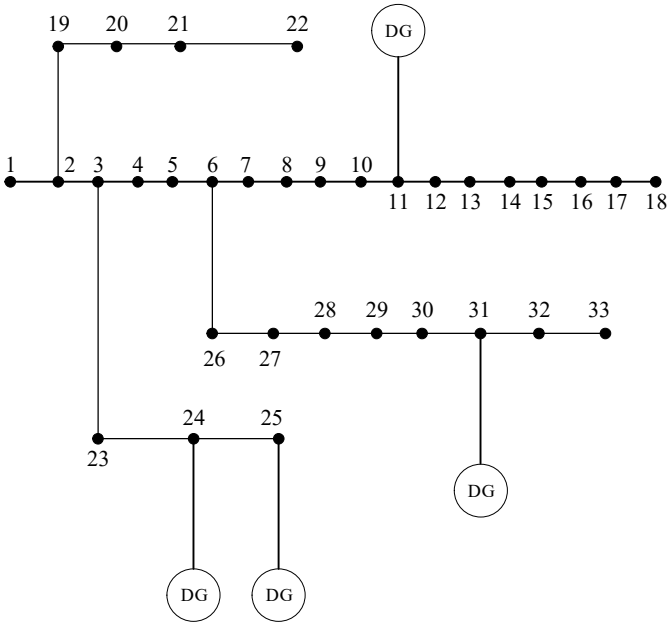


Figure 9: DG access location based on IPSO algorithm

Table 1: Parameter comparison after the system is connected to DG

| Algorithm | DG access node | Access capacity/MW | Disconnect the branch road | Voltage deviation /p.u | Network loss kW |
|---|---|---|---|---|---|
| PSO | 28,14,17,11 | 1,0.61,0.52,0.58 | 7,14,10,31,28 | 0.27736 | 63.884 |
| IPSO | 31,24,11,25 | 0.95,0.95,0.95,0.95 | 33,14,8,16,28 | 0.17008 | 59.782 |

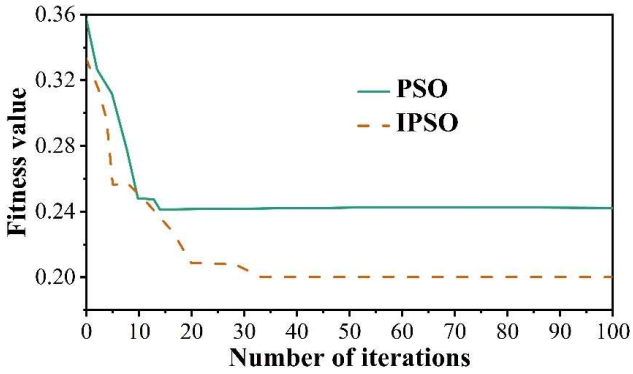


Figure 10: Iterative convergence comparison

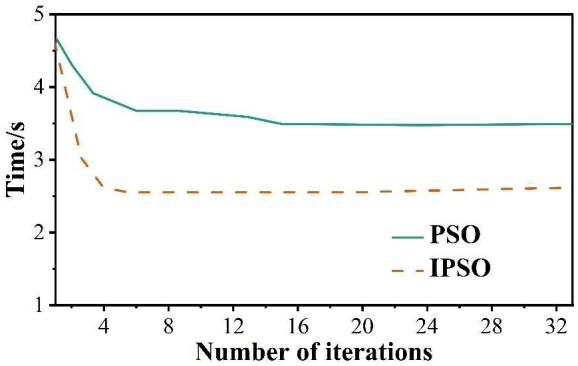


Figure 11: Comparison of protection coordination time

Table 2: Optimize the coordination effect of system protection before and after

| N | Before | | After | |
|---|---|---|---|---|
| | Current/A | Voltage/V | Current/A | Voltage/V |
| 1 | 26.47856 | 398.56751 | 20.23379 | 376.59406 |
| 2 | 29.75606 | 403.78368 | 20.39814 | 379.3401 |
| 3 | 25.07056 | 414.66747 | 20.40424 | 384.27562 |
| 4 | 25.69084 | 414.71716 | 19.43843 | 381.81344 |
| 5 | 25.39685 | 403.55507 | 20.53394 | 380.74355 |
| 6 | 24.64535 | 402.36778 | 20.56098 | 379.82614 |
| 7 | 22.90045 | 388.35264 | 20.24373 | 375.05493 |
| 8 | 20.37378 | 403.87916 | 20.31529 | 377.34032 |
| 9 | 24.74598 | 384.84461 | 20.02338 | 378.49945 |
| 10 | 24.56788 | 394.66504 | 20.50694 | 382.26042 |
| 11 | 24.33713 | 379.51772 | 20.06764 | 383.0355 |
| 12 | 27.93709 | 410.06576 | 19.70211 | 381.21935 |
| 13 | 26.19096 | 381.09874 | 19.22989 | 378.5133 |
| 14 | 27.19069 | 385.49592 | 20.0763 | 377.21531 |
| 15 | 26.60517 | 390.74091 | 19.81349 | 380.92802 |
| 16 | 24.56448 | 401.22422 | 20.40933 | 379.31717 |
| 17 | 27.94331 | 403.10401 | 20.22056 | 377.64047 |
| 18 | 25.87591 | 401.75723 | 20.49462 | 384.25865 |
| 19 | 26.2739 | 414.20655 | 19.43401 | 378.28742 |
| 20 | 22.51715 | 406.33523 | 20.13709 | 378.19349 |
| 21 | 20.73868 | 404.24038 | 19.88456 | 385.14778 |
| 22 | 25.02903 | 399.83997 | 19.49192 | 381.55926 |
| 23 | 26.21646 | 409.34529 | 20.09881 | 376.83647 |
| 24 | 26.67467 | 412.6934 | 19.52425 | 381.51683 |
| 25 | 24.46025 | 401.23621 | 20.04523 | 380.33552 |
| 26 | 23.82058 | 395.7591 | 19.65647 | 377.47158 |
| 27 | 24.87386 | 373.67576 | 20.79204 | 379.7152 |
| 28 | 24.38835 | 392.97047 | 19.4554 | 379.44387 |
| 29 | 23.32812 | 385.47584 | 19.78378 | 378.20251 |
| 30 | 23.38714 | 405.4421 | 19.78439 | 379.0357 |

### *IV. C. Practical case studies*

#### IV. C. 1) Overview of cases

The Tian-Guang ±500 kV DC transmission project is an AC-DC parallel operation system, which was put into operation in June 2001 at both poles, thus making the Southern Power Grid a large grid with AC-DC parallel operation. In this paper, we mainly consider the C grid as an example, in which the C grid sends power out to the D grid through the Rome line and the Luma line, and sends power to Guangdong through the Tianguang DC. In order to consider the parallel operation condition of AC and DC, the system is simplified and equalized. The C grid is considered in detail in the calculation, the D and E grids are considered as their main units, and the Guangdong grid is equaled to the first class value machine. Taking the system operation mode as an example, the simplified system has 29 generators. Among them, there are 18 units in C grid, 2 units in D grid, 2 units in Tianshengqiao I, 3 units in Tianshengqiao II and 3 units in E grid. In this operation mode, the DC line sends 720 MW to the southern grid, and the corresponding parameters of the generators and excitation system are taken from the manual.

#### IV. C. 2) Analysis of protection coordination effects

Using the model of this paper to optimize the above case, the current (normal state value of 20A) and voltage (normal state value of 380V) of 30 system devices are used as the basis for judging the analysis of protection coordination effect, and the analysis of system protection coordination effect before and after optimization is shown in Table 2. As can be seen from the values in the table, when the system is not introduced into the model of this paper, the values of the equipment current and voltage are 20-28A and 370V-415V, reflecting the unstable operation of the equipment of the AC-DC hybrid power system. After the protection and coordination of this model, the current and voltage values of the system equipment are 19~21A, 370~390V, and the error of the normal state is kept below

5%, which indicates that after the introduction of this model, the operation of the equipment of the AC/DC hybrid power system is more stable, and it further proves the protection and coordination of this model, which can make the AC/DC power system serve the users better.

## V. Conclusion

In this paper, combined with the relevant knowledge of electrical theory, the AC/DC hybrid power system is divided into AC system and DC system, and the relevant regulator, stabilizer, filter, controller and rectifier are used to complete the task of constructing the AC/DC hybrid power system. Based on the knowledge of distributed computing theory, the system multi-area protection coordination problem is converted into a mixed integer nonlinear programming problem, and the objective function, constraints, and optimization model solution algorithms are determined to finally complete the design work of the system multi-area protection coordination scheme. According to the above algorithms and models, the multi-area protection coordination of AC-DC hybrid power system is empirically analyzed. Through the test function to verify the optimization performance of this paper's algorithm, it is found that the optimization performance of this paper's algorithm is more ideal, and its optimal solution is more in line with the actual situation of the system. In addition, this paper's algorithm calculates the optimal solution of the protection coordination time of the system after connecting to the DG with the value of 2.531s, which further optimizes the protection coordination time of the system and guarantees the stable operation of the system equipment. In order to make the research results more persuasive, the system protection coordination case study is also added, after the model of this paper, the current and voltage values of the system equipment are stabilized at 19~21A, 370~390V, with an error of less than 5%, which is completely within the permissible range of the system, so as to maintain the normal operation of the system, and to provide reference for the intelligent diagnosis and coordination of AC/DC hybrid power systems.

## Funding

This work was supported by the Supporting Special Topic 9 of Guangdong's "15th Five Year Plan" New Power System Planning: Research on Guangdong Power Grid's "15th Five Year Plan" Secondary System Planning (Project Number: 031000QQ00240021).

## References

[1] Chaudhary, S. K., Guerrero, J. M., & Teodorescu, R. (2015). Enhancing the capacity of the AC distribution system using DC interlinks—A step toward future DC grid. IEEE Transactions on Smart Grid, 6(4), 1722-1729.

[2] Mohammed, S. A. Q., & Jung, J. W. (2021). A state-of-the-art review on soft-switching techniques for DC–DC, DC–AC, AC–DC, and AC–AC power converters. IEEE Transactions on Industrial Informatics, 17(10), 6569-6582.

[3] Gelani, H. E., Dastgeer, F., Nasir, M., Khan, S., & Guerrero, J. M. (2021). AC vs. DC distribution efficiency: Are we on the right path?. Energies, 14(13), 4039.

[4] Gerber, D. L., Vossos, V., Feng, W., Marnay, C., Nordman, B., & Brown, R. (2018). A simulation-based efficiency comparison of AC and DC power distribution networks in commercial buildings. Applied Energy, 210, 1167-1187.

[5] Dastgeer, F., & Gelani, H. E. (2017). A Comparative analysis of system efficiency for AC and DC residential power distribution paradigms. Energy and Buildings, 138, 648-654.

[6] Gerber, D. L., Vossos, V., Feng, W., Khandekar, A., Marnay, C., & Nordman, B. (2017, June). A simulation based comparison of AC and DC power distribution networks in buildings. In 2017 IEEE Second International Conference on DC Microgrids (ICDCM) (pp. 588-595). IEEE.

[7] Zhang, L., Liang, J., Tang, W., Li, G., Cai, Y., & Sheng, W. (2018). Converting AC distribution lines to DC to increase transfer capacities and DG penetration. IEEE Transactions on Smart Grid, 10(2), 1477-1487.

[8] Montoya, O. D., Serra, F. M., & De Angelo, C. H. (2020). On the efficiency in electrical networks with AC and DC operation technologies: A comparative study at the distribution stage. Electronics, 9(9), 1352.

[9] Navarro-Rodriguez, A., Garcia, P., Georgious, R., & García, J. (2018). Adaptive active power sharing techniques for DC and AC voltage control in a hybrid DC/AC microgrid. IEEE Transactions on industry applications, 55(2), 1106-1116.

[10] Liu, X., Liu, Y., Liu, J., Xiang, Y., & Yuan, X. (2019). Optimal planning of AC-DC hybrid transmission and distributed energy resource system: Review and prospects. CSEE Journal of Power and Energy Systems, 5(3), 409-422.

[11] Sahoo, S. K., Sinha, A. K., & Kishore, N. K. (2017). Control techniques in AC, DC, and hybrid AC–DC microgrid: A review. IEEE Journal of Emerging and Selected Topics in Power Electronics, 6(2), 738-759.

[12] Zhu, D., Cheng, W., Duan, J., Wang, H., & Bai, J. (2023). Identifying and assessing risk of cascading failure sequence in AC/DC hybrid power grid based on non-cooperative game theory. Reliability Engineering & System Safety, 237, 109359.

[13] Dong, X., Guan, E., Jing, L., Wang, H., & Mirsaeidi, S. (2020). Simulation and analysis of cascading faults in hybrid AC/DC power grids. International Journal of Electrical Power & Energy Systems, 115, 105492.

[14] Mehdi, A., Hassan, S. J. U., Haider, Z., Arefaynie, A. D., Song, J. S., & Kim, C. H. (2024). A systematic review of fault characteristics and protection schemes in hybrid AC/DC networks: Challenges and future directions. Energy Reports, 12, 120-142.

[15] Sun, P., Teng, Y., Zhang, M., & Chen, Z. (2021). A novel risk assessment method for hybrid AC/DC system based on transient energy function. CSEE Journal of Power and Energy Systems.

[16] Monadi, M., Zamani, M. A., Candela, J. I., Luna, A., & Rodriguez, P. (2015). Protection of AC and DC distribution systems Embedding distributed energy resources: A comparative review and analysis. Renewable and sustainable energy reviews, 51, 1578-1593.

[17] Shahzad, U., Kahrobaee, S., & Asgarpoor, S. (2017). Protection of distributed generation: challenges and solutions. Energy and Power Engineering, 9(10), 614-653.
[18] Ionuţ Gabriel Farcaş,Rayomand P. Gundevia,Ramakanth Munipalli & Karen E. Willcox. (2025). Distributed computing for physics-based data-driven reduced modeling at scale: Application to a rotating detonation rocket engine. Computer Physics Communications,313,109619-109619.
[19] Preeti Chaudhary,Satvik Vats & Vikrant Sharma. (2025). Performance Insights of Convolutional Neural Networks Operating on Distributed Computing Platforms. SN Computer Science,6(4),371-371.